iScience

CellPress
OPEN ACCESS

Article

Manipulation of ion/electron carrier genes in the model diatom *Phaeodactylum tricornutum* enables its growth under lethal acidic stress

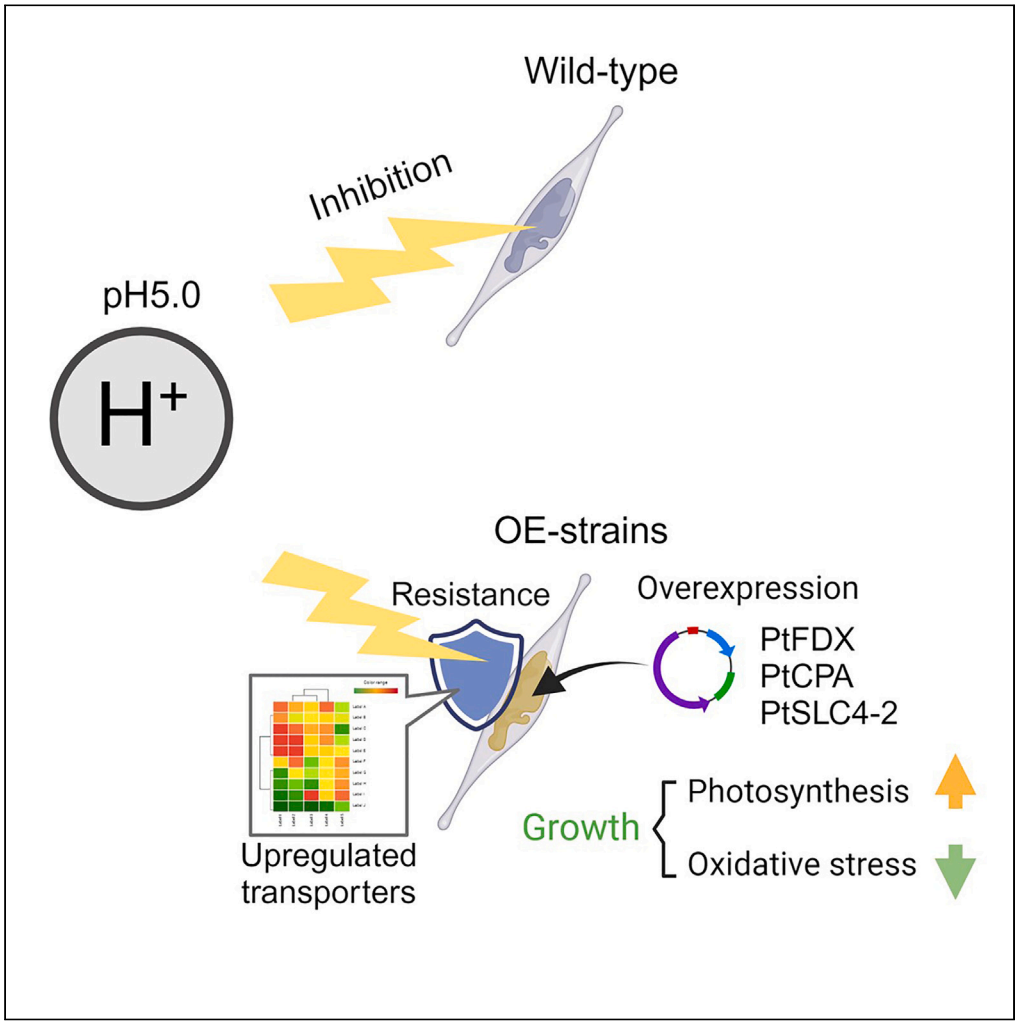

Yixi Su, Jiwei Chen, Jingyan Hu, Cheng Qian, Jiahao Ma, Sigurður Brynjolfsson, Weiqi Fu

weiqifu@zju.edu.cn

Highlights

Manipulating ion/electron carrier genes enables algal growth under lethal pH levels

Enhanced PtCPA and PtSCL4-2 upregulate the expression of transmembrane transporters

Increased acid resistance boosts algal photosynthesis with reduced oxidative stress

Su et al., iScience 27, 110482
August 16, 2024
https://doi.org/10.1016/j.isci.2024.110482

iScience

CellPress
OPEN ACCESS

Article

Manipulation of ion/electron carrier genes in the model diatom *Phaeodactylum tricornutum* enables its growth under lethal acidic stress

Yixi Su,[1,2] Jiwei Chen,[1] Jingyan Hu,[1] Cheng Qian,[1,3] Jiahao Ma,[1] Sigurður Brynjolfsson,[2] and Weiqi Fu[1,2,4,*]

SUMMARY

A major obstacle to exploiting industrial flue gas for microalgae cultivation is the unfavorable acidic environment. We previously identified three upregulated genes in the low-pH-adapted model diatom *Phaeodactylum tricornutum*: ferredoxin (PtFDX), cation/proton antiporter (PtCPA), and HCO_3^- transporter (PtSCL4-2). Here, we individually overexpressed these genes in *P. tricornutum* to investigate their respective roles in resisting acidic stress (pH 5.0). The genetic modifications enabled positive growths of transgenic strains under acidic stress that completely inhibited the growth of the wild-type strain. Physiological studies indicated improved photosynthesis and reduced oxidative stress in the transgenic strains. Transcriptomes of the PtCPA- and PtSCL4-2-overexpressing transgenics showed widespread upregulation of various transmembrane transporters, which could help counteract excessive external protons. This work highlights ion/electron carrier genes' role in enhancing diatom resistance to acidic stress, providing insights into phytoplankton adaptation to ocean acidification and a strategy for biological carbon capture and industrial flue gas CO_2 utilization.

INTRODUCTION

The Intergovernmental Panel on Climate Change (IPCC, the United Nations body for assessing the science related to climate change), has determined that carbon dioxide (CO_2) missions due to the consumption of fossil fuels significantly contribute to global warming.[1] In this context, algal biotechnology driven by the imperative to reduce CO_2 footprint can benefit various sectors such as environment management and sustainable production of renewable fuels, food, and chemicals for a bio-based economy.[2] To maximize economic profitability while mitigating CO_2 emissions, integration of microalgae production into greenhouse gas (GHG) emitting industries is desirable, as it allows for the creation of value-added products using untapped carbon in industrial flue gas. However, challenges associated with flue gas, such as the inhibitory effect of acidic pH on algal growth, must be addressed prior to microalgae-based manufacturing.[3] Depending on flue types, flue gas from combustion processes could contain complex constituents, including CO_2, NO_x, SO_x, CO, C_xH_x, particular matter (PM), heavy metals, etc.[4] The presence of acidic gases, typically 10%–20% CO_2 and small amounts of SO_x and NO_x, can lead to extremely acidic pH conditions, reaching as low as 2,[5,6] which causes severe inhibition on photosynthesis and thus algal growth.[7] In addition to process optimization aimed at alleviating cultivation stresses,[8,9] efforts have been made to isolate tolerant algal strains.[10] *Chlorella* sp. and *Scenedesmus* sp. have shown the most robust growth in cultivation using flue gas.[11]

Moreover, strain improvement strategies including random mutagenesis,[12] adaptive laboratory evolution (ALE),[13,14] and genetic engineering[15] have been employed to enhance microalgae productivity under unfavorable environments. For instance, chemical mutagenesis followed by stress exposure was applied to generate *Chlorella* mutants with improved thermotolerance[16] and alkali tolerance.[17] ALE techniques have yielded *Chlorella* sp. with high-CO_2 tolerance,[11] *Picochlorum* sp. with improved thermotolerance,[18] and *Phaeodactylum tricornutum* strains with low-pH tolerance,[19] all exhibiting enhanced growth under stressful conditions. Moreover, *Chlamydomonas reinhardtii* was genetically modified to overexpress a heterologous pyrroline-5-carboxylate synthetase, resulting in elevated intracellular proline levels and improved tolerance to toxic heavy metals.[20] The introduction of green alga plastocyanin that provides alternative redox couples has been reported to improve the growth of *P. tricornutum* in iron-deficient conditions.[21] A recent study modified fatty acid compositions in *P. tricornutum* by overexpressing a 3-oxoacyl acyl carrier protein reductase, which led to enhanced thermotolerance in the transgenic strains.[22]

P. tricornutum is a model species of marine diatoms featured by efficient photosynthetic conversion of inorganic CO_2 into biomass and high yields of lipids, carotenoids, and protein, which position it as a promising cellular factory.[23] Besides the availability of the published

[1]Ocean College, Zhejiang University, Zhoushan, Zhejiang 316021, China
[2]Center for Systems Biology and Faculty of Industrial Engineering, School of Engineering and Natural Sciences, University of Iceland, 101 Reykjavík, Iceland
[3]School of Biological Sciences, The University of Hong Kong, Hong Kong SAR, China
[4]Lead contact
*Correspondence: weiqifu@zju.edu.cn
https://doi.org/10.1016/j.isci.2024.110482

genomic sequence,[24] *P. tricornutum* benefits from well-established molecular techniques for transformation, gene overexpression, silencing, and knockout, enabling targeted trait engineering and reverse genetic investigations of gene functions.[25] Over the past decades, there has been extensive research on the metabolic networks of *P. tricornutum*, focusing on optimizing carbon fluxes to increase the accumulation of specific metabolites, particularly lipids, and carotenoids.[26–28] Additionally, a limited number of studies have explored strategies to increase biomass production by manipulating the C4 pathway and pyruvate transportation.[29,30] One recent study reported that the pH tolerance of *C. reinhardtii* was enhanced through overexpression of an H^+-ATPase pump.[15] However, research on genetic manipulation to improve microalgal growth under environmental stress has been obscure.

To investigate the acidic stress that is likely to be encountered in industrial production with flue gas as well as ocean acidification, we previously applied ALE to domesticate low-pH tolerant strains of *P. tricornutum* and studied their adaptive responses to acid exposure in long-term semi-continuous cultivation.[19] Common differentially expressed genes (DEGs) were identified in three independently evolved cultures, indicating the significance of the photosynthetic electron transport chain (ETC), proton transporters, and bicarbonate transporters in conferring acidic tolerance.[19] In particular, substantial upregulation of three genes with gene identifiers (IDs) of Phatr3_J33543, Phatr3_J50516, and Phatr3_Jdraft1806 was identified in all culture adapted to low-pH conditions. Phartr3_J33543 and Phatr3_J50516 are predicted proteins that likely possess conserved polypeptide domains associated with electron transfer activity and solute:proton antiporter activity, respectively. Phatr3_Jdraft1806 has previously been identified as a solute carrier 4 (SLC4) gene responsible for HCO_3^- transport.[31]

The ion/electron carrier genes and their products have the potential to influence cellular proton homeostasis, thereby contributing to pH adaptation in diatoms. During photosynthesis, captured light energy is converted into chemical energy via ETCs. Ferredoxins (FDXs) containing an [2Fe-2S] active center are the soluble electron transport proteins that mediate linear electron transfer (LET) and cyclic electron transfer (CET). These processes generate proton gradients across the thylakoid membrane to drive adenosine triphosphate (ATP) synthesis.[32] Additionally, FDXs can shuttle excess electrons produced during photosynthesis to other metabolic processes such as carbon and nitrogen assimilation, thereby promoting microalgal growth. Studies have shown that overexpression of FDXs can reduce cellular levels of reactive oxygen species (ROS) and improve stress tolerance in green microalgae.[33,34] Moreover, the product of Phatr3_J50516 containing a cation/proton antiporter (CPA) domain belongs to a class of Na^+/H^+ antiporter. CPAs directly regulate pH homeostasis and levels of cation ions such as K^+, Na^+, and Ca^{2+}, which could indirectly participate regulation of photosynthesis, protein metabolism, and stress responses, as well as plant growth and development.[35,36] While the role of Na^+/H^+ antiporters in salt stress resistance has been fully demonstrated in plants,[37,38] it has been shown that Na^+/H^+ antiporters are essential for maintaining the internal pH homeostasis in bacteria under extreme extracellular pH conditions.[39–41] Finally, SLC4 involving a CO_2-concentrating mechanism (CCM) plays a vital role in the adaptation of diatoms to low-carbon availability environments. HCO_3^- uptake not only helps regulation of pH homeostasis by providing buffering capacity against acidified conditions but also enhances carbon concentrating in a low-pH environment where total dissolved inorganic carbon (DIC) is reduced.[42] Despite the well-established understanding of the localization and catalytic properties of PtSLC4-2 and its paralogs (PtSLC4-1 and PtSLC4-4),[31,43] the impact of these bicarbonate transporters on the low-pH tolerance in microalgae remains unclear, although evidence of intracellular pH regulation by SLC4 family has been widely reported in animal cells.[44–46]

Here we investigated the potential roles of three ion/electron carrier genes (Phatr3_J33543, Phatr3_J50516, and Phatr3_Jdraft1806) in the model diatom *P. tricornutum* regarding their involvement in low-pH adaptation. We achieved this by constructing transgenic strains and assessing their physiological and transcriptomic profile changes. Furthermore, this study represents the first attempt to rationally engineer diatoms to enable cell growth and carbon fixation under inhibitory acidic stress, which could provide critical insights into gene regulations involved in microalgal response to acidic stress as well as ocean acidification.

RESULTS

Construction of transgenic *P. tricornutum*

Based on our previous study, the expression of three genes (Phatr3_J33543, Phatr3_J50516, and Phatr3_Jdraft1806) was outstandingly enhanced (1.6- to 36.5-fold compared to corresponding genes in the wild type [WT]) in all the evolved strains that had been acclimated in acidic conditions (Table S1).[19] The Phatr3_J33543 protein contains an FDX domain and a PDZ domain. Phylogenetic analysis indicated that the FDX domain is widely conserved among diatoms and cyanobacteria, but the PDZ domain is unique to diatoms (Figure S1A). Furthermore, the proteins encoded by Phatr3_J50516 and Phatr3_Jdraft1806 exhibit conserved domains across various diatom species (Figures S1B and S1C).

The present study attempted to overexpress these genes in *P. tricornutum* to investigate their roles in conferring low-pH tolerance. The coding sequence of each gene was tagged with an enhanced green fluorescence protein (EGFP) gene (Figure 1A). Multiple transgenic lines were generated for each construct, and subsequent selection was based on green fluorescence intensity compared to the WT and growth rates (Figure S2). Three lines (designated as PtFDX-OE10, PtCPA-OE21, and PtSLC-OE31, corresponding to clone #10 for Phatr3_J33543, clone #21 for Phatr3_J50516, clone #31 for Phatr3_Jdraft1806, respectively) exhibited the strongest EGFP signal were selected for further characterization.

The presence of recombinant genes in transgenics was determined by genomic PCR amplifying a fragment spanning the transgene::EGFP fusion (Figure 1B). Successful expression of recombinant proteins in the transgenic strains was confirmed by detecting their green fluorescence signals which were 5- to 10-fold of that in the WT (Figure 1C). Visualization of EGFP through fluorescent microscopy (Figure 1D) revealed subcellular localization of the recombinant proteins in various organelles. Notably, the PtFDX protein encoded by Phatr3_J33543 exhibited

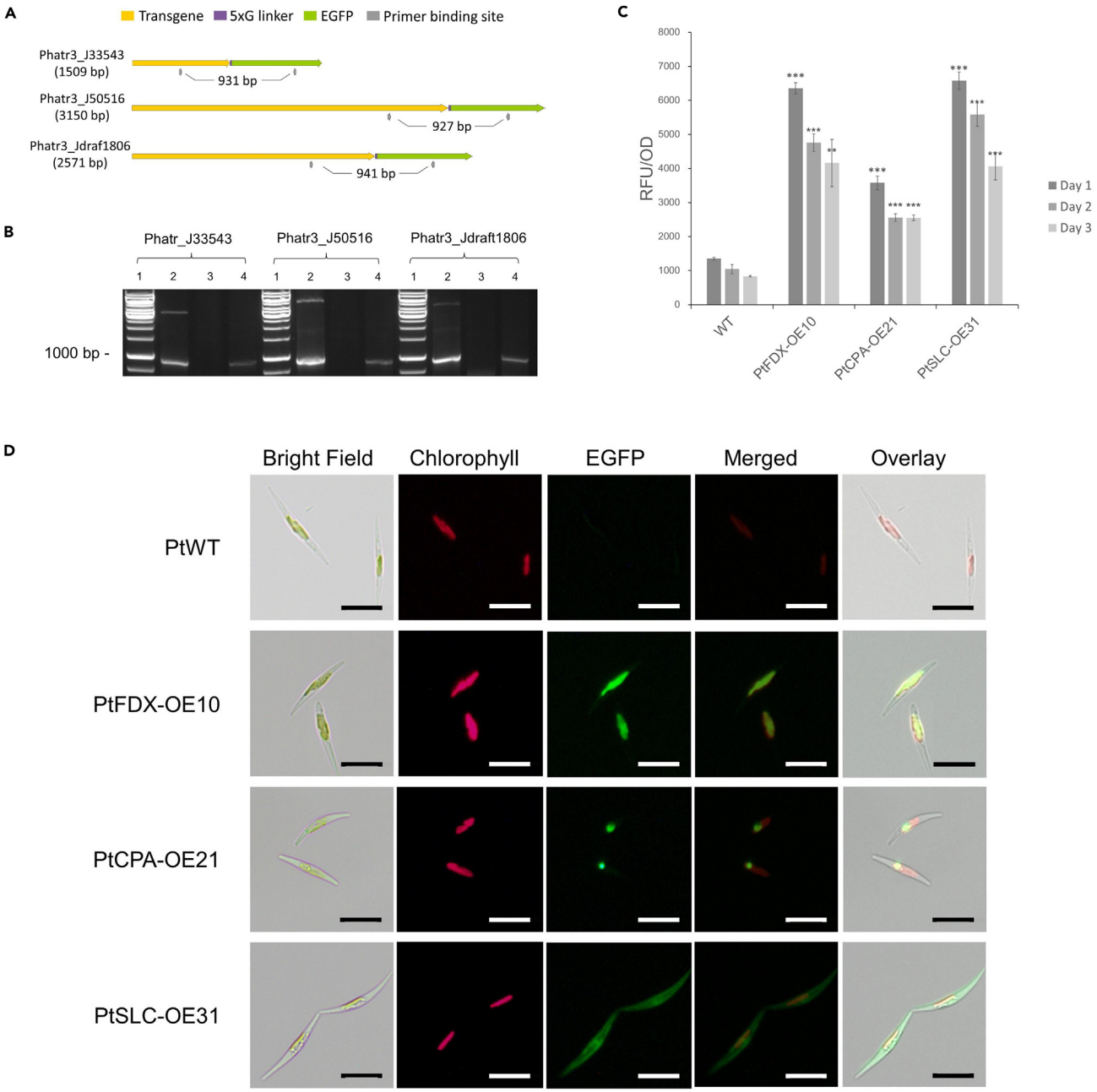

Figure 1. Construction of Transgenic *P. tricornutum* overexpressing recombinant genes

(A) Recombinant gene constructs. Phatr3_J33543 encodes a ferredoxin (FDX); Phatr3_J50516 encodes a cation/proton antiporter (CPA); Phatr3_Jdraft1806 encodes a solute carrier HCO_3^- transporter (SLC); EGFP stands for enhanced green fluorescence protein.

(B) PCR analysis of the recombinant gene using genomic DNA as a template. For each transgeneEGFP fusion, lane 1, ladder; lane 2, plasmid (positive control); lane 3, WT; lane 4, transgenic strain.

(C) Normalized green fluorescence intensity in the seed culture over three successive days after inoculation (excitation wavelength of 488 nm and emission wavelength of 525 nm). Data are represented as mean ± standard deviation (n = 3); NS, $p > 0.05$; *$p < 0.05$; **$p < 0.01$; ***$p < 0.001$ (Student's t test). RFU, relative fluorescence unit; OD, optical density.

(D) Fluorescence microscopic images of wild-type *P. tricornutum* (PtWT) and overexpression transgenic strains (PtFDX-OE10, PtCPA-OE21 and PtSLC-OE31) (scale bar indicates 10 μm).

expression throughout the entire chloroplast, while the proton transporter encoded by Phatr3_J50516 was confined to a small compartment within the chloroplast. As for PtSLC4-2 encoded by Phatr3_Jdraft1806, EGFP was distributed in the cytosol but was intensified at the plasma membrane, consistent with previous findings.[31]

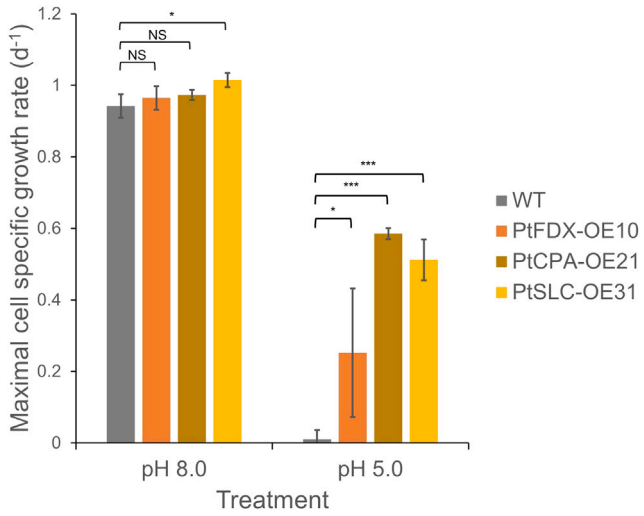

Figure 2. Growth characterization of different strains under low-pH treatments

Different strains were cultivated at pH 8.0 for 5 days and then transferred into acidic enriched artificial seawater (EASW) media (pH 5.0) in identical conditions (40 μmol m^{-2} s^{-1} red/blue LED, 22 ± 1°C) for the low-pH treatments. PtFDX-OE10, PtCPA-OE21, and PtSLC-OE31 are genetically modified strains with overexpressed ferredoxin (Phatr3_J33543), cation/proton antiporter (Phatr3_J50516), and bicarbonate transporter (Phatr3_Jdraft1806). Data are represented as mean ± standard deviation (n = 3). NS, $p > 0.05$; *$p < 0.05$; **$p < 0.01$; ***$p < 0.001$ (Student's t test).

Growth rate and photosynthetic efficiency at inhibitory pH

The selected PtFDX-OE10, PtCPA-OE21, and PtSLC-OE31 transformants were subjected to growth experiments at pH 8.0 (control), pH 5.5, and pH 5.0. The maximal specific rates were determined at 24 h for all experiments (Figure 2). At a favorable pH for diatom growth (pH 8.0), the growth rates of all tested strains were comparable, though PtSLC-OE31 exhibited a slightly higher maximal growth rate than the WT ($p < 0.05$) (Figure 2). The promotive effect of overexpressing PtSLC4-2 on DIC uptake and photosynthesis could account for the slight growth increase observed in PtSLC-OE31.[31] Notably, significant differences between transgenic strains and the WT were observed until decreasing pH 5.0 that led to a pronounced growth inhibition in the WT (Figure S3). In contrast to the dying WT, all three transformants showed positive growths at 24 h, although the low-pH stress resulted in 73.8%, 39.9%, and 49.6% reduction in maximal growth rate of PtFDX-OE10, PtCPA-OE21, and PtSLC-OE31, respectively (Figure 2). However, the growths of transgenic strains ceased after 24 h. While PtFDX-OE10 experienced a decline after 24 h, the cell densities of PtCPA-OE21 and PtSLC-OE31 remained static without significant changes over the following four days (Figure S3).

At pH 8.0, photosynthetic parameters showed similar trends in both the WT and transformants (Figure 3). The maximal quantum yield (Fv/Fm) remained consistently high (>0.6) throughout the cultivation, indicating a non-stressed environment. While effective quantum yield (Φ_{PSII}) peaked at 24 h and declined afterward, the non-photochemical quenching (NPQ) parameter increased gradually from 48 h until the end of the experiment. These results suggest that photosynthetic efficiency decreased with the growth of cell density, likely due to the shading effect. As the energy dissipation through heat and fluorescence increased, the proportion of harvested energy used for biomass growth decreased. Following the transfer to the pH 5.0 media, the Fv/Fm values in all three transgenic strains exhibited a significant decline within 24 h, indicating a pronounced inhibition of photosynthesis caused by the serious acidic stress. Nevertheless, the Fv/Fm values in transformants were significantly higher than those in the WT ($p < 0.05$), suggesting a relatively reduced stress in reflection of survival of transgenic strains under low-pH conditions. Similarly, Φ_{PSII} decreased to extremely low levels, corresponding to halted growth in all cultures. Notably, the NPQ in WT was consistently maintained at a relatively low level throughout the cultivation, whereas this parameter substantially increased in transgenic strains after 24 h and then decreased to a level comparable to that of the WT.

Oxidative stress under low-pH treatment

Intracellular ROS levels were monitored to assess the effects of medium pH on cell physiological status. In pH 8.0 media, the intracellular ROS levels in all three transgenic strains were increased after inoculation and gradually decreased as acclimation. Upon acidic treatment, intracellular ROS in the WT was significantly higher than that in the transformants. While WT cells underwent continuously increasing intracellular ROS, the ROS levels in transformants were maintained relatively low (Figure 4A). These results indicate that transgenic strains were less stressed compared to the WT when growing at pH 5.0. Furthermore, superoxide dismutase (SOD) activities in PtCPA-OE21 and PtSLC-OE31 were relatively stable over cultivation. The antioxidant defense in WT and HI33543 showed an increasing tendency (Figure 4B), which is correlated with the relatively high ROS levels in these strains.

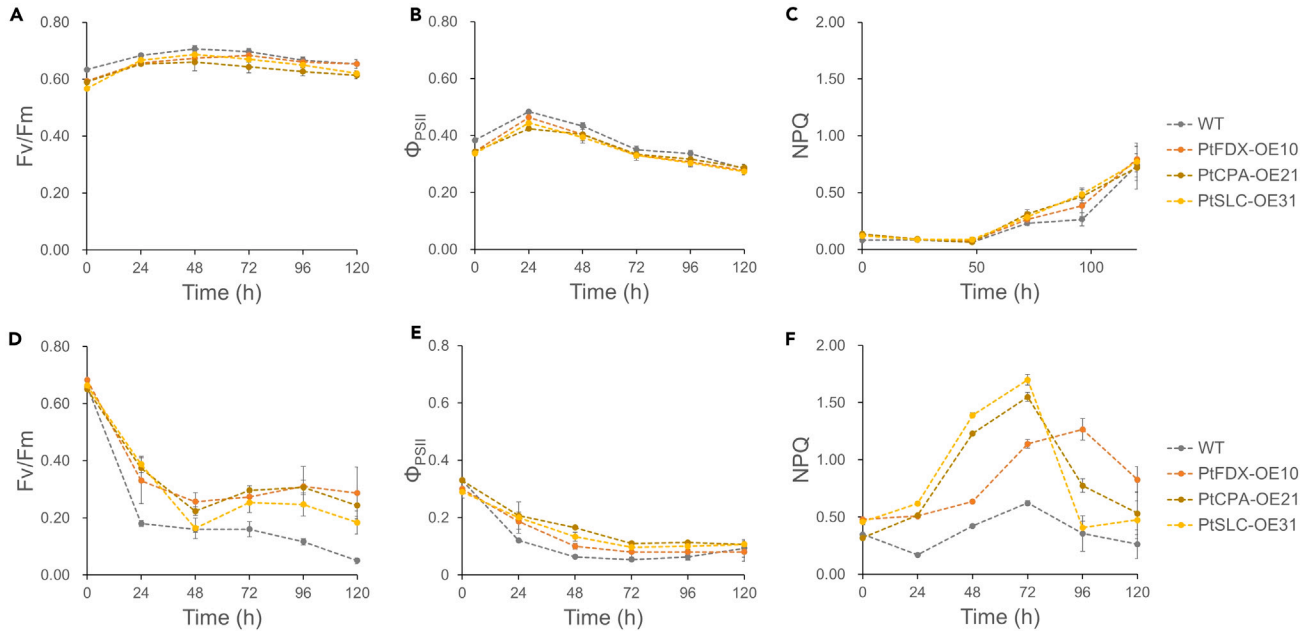

Figure 3. Effects of iow pH treatment on photosynthetic performance in different strains

Different strains were cultivated at pH 8.0 for 5 days and then transferred into acidic EASW media (pH 5.0) in identical conditions (40 μmol m^{-2} s^{-1} red/blue LED, 22 ± 1°C). PtFDX-OE10, PtCPA-OE21, and PtSLC-OE31 are genetically modified strains with overexpressed ferredoxin (Phatr3_J33543), cation/proton antiporter (Phatr3_J50516), and bicarbonate transporter (Phatr3_Jdraft1806).

(A–C) Photosynthetic parameters at pH 8.0 (A) Fv/Fm, (B) Φ_{PSII}, and (C) NPQ.

(D–F) Photosynthetic parameters at pH 5.0(A) Fv/Fm, (B) Φ_{PSII}, and (C) NPQ. Fv/Fm, maximal quantum yield of photosystem II. Φ_{PSII}, effective quantum yield for photochemistry. NPQ, non-photochemical quenching. Data are represented as mean ± standard deviation (n = 3). Two-factorial ANOVA was used to analyze photosynthesis parameters, showing significant differences ($p < 0.05$) among different strains.

Effect of low-pH stress on gene expression

A transcriptomic study was conducted to investigate molecular responses to acidic pH in diatoms and the underlying mechanisms that could contribute to improved low-pH tolerance. For all three transgenic strains, samples were collected at the starting point from the inoculum culture (pH 8.0) and at 24 h after the low-pH treatment (pH 5.0). The principal-component analysis (PCA) showed distinct clusters between samples at 0 h and 24 h, but different strains under the same pH conditions were less distinguishable (Figure 5A).

As for the transcriptomic responses to low pH (24 h/0 h), 4,641, 5,589, 3,638, and 5,221 DEGs were identified in WT, PtFDX-OE10, PtCPA-OE21, and PtSLC-OE31, respectively (Figure 5B). Upregulated and downregulated DEGs were separately subjected to the Gene Ontology (GO) enrichment analysis that resulted in 34, 26, 52, and 25 significantly enriched GO terms ($P_{adj} < 0.05$) for WT, PtFDX-OE10, PtCPA-OE21, and PtSLC-OE31, respectively. Based on a greedy search strategy, driver terms were generated presenting at least one function from each connected component[47] (Figure 5D). The WT and transgenic strains with different genetic bases differed in their gene expression responses to acidic. Nevertheless, 11 enriched GO terms that mostly related to photosynthesis (GO:0015979) were shared in all the strains in a down-regulation pattern, including chlorophyll-binding proteins (GO:0016168, GO:0009765, GO:0019684) and chlorophyll biosynthetic processes (GO:0033014, GO:0006778) (Figure 5C). Further investigation on the underrepresented terms revealed commonly upregulated functions relating to protein transport/repair/degradation/translation (GO:0009987, GO:0046907, GO:0043043, GO:0006412) and regulation of gene expression (GO:0010467).

Considering potential mechanisms involving acidic responses including oxidative stress, proton pumping, and energy supply, we explored annotated genes encoding peroxidases, ATP binding cassette (ABC) transporters, P-type ATPases, and tricarboxylic acid cycle (TCA) enzymes. It was found that the glutathione redox cycle including glutathione peroxidase (GPx), glutathione reductase (GR), and glutathione S-transferase was provoked by the acidic stress in WT and PtFDX-OE10 (Figure 5E). Nevertheless, the glutathione metabolism in PtCPA-OE21 and PtSLC-OE31 showed different expression patterns with many genes remaining unchanged or downregulated (Figure 5E). In all three transgenic strains, expression of a catalase-peroxidase (Phatr3_J18572) and an L-ascorbate peroxidase (APX) (Phatr3_J54731) was substantially increased by 2.5- to 61.8-fold and 2.9- to 4.4-fold, respectively, but APX genes were found generally downregulated. P-type adenosine triphosphatase (P-ATPases) and ABC transporters are the two principal active transporters in organisms. For these genes, the ratios of identified upregulated/downregulated genes were 3/9, 5/6, 6/0, and 9/4 in WT, PtFDX-OE10, PtCPA-OE21, and PtSLC-OE31, respectively, which implies stimulated active transportation in PtCPA-OE21 and PtSLC-OE31. Notably, considerable upregulation (2.1- to 11.2-fold) of an ABC transporter (Phatr3_J14778) and a P-type ATPase (Phatr3_EG02611) was observed in all three transgenic strains. As expected,

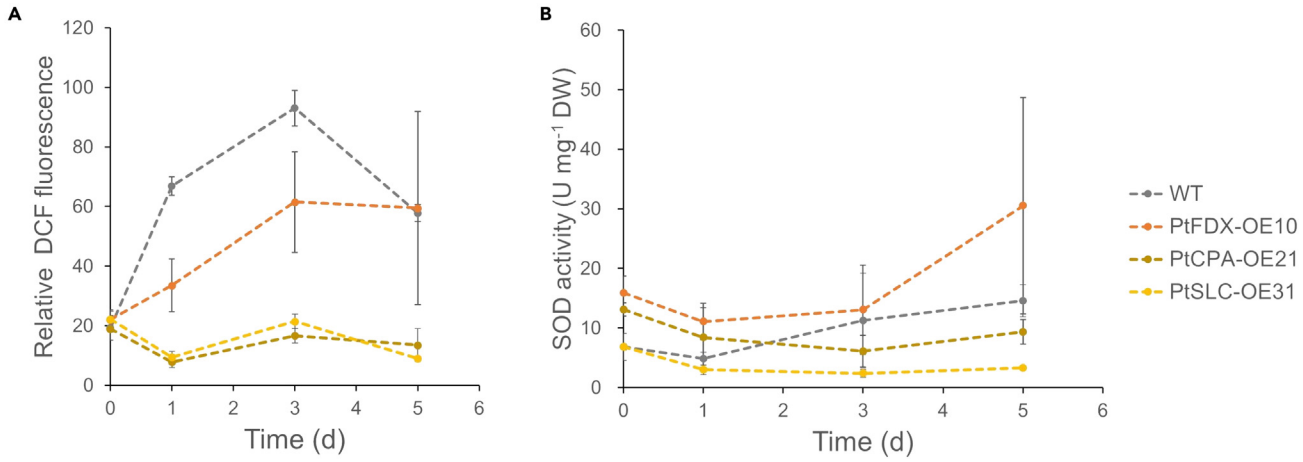

Figure 4. Intracellular oxidative stress and antioxidant capacity assessment

Seed cultures of different strains were grown at pH 8.0 for 5 days and then transferred into acidic EASW media (pH 5.0) in identical conditions (40 μmol m^{-2} s^{-1} red/blue LED, 22 ± 1°C). Oxidative stress and SOD activity during the low-pH treatment were monitored on days 0, 1, 3, and 5. PtFDX-OE10, PtCPA-OE21, and PtSLC-OE31 are genetically modified strains with overexpressed ferredoxin (Phatr3_J33543), cation/proton antiporter (Phatr3_J50516), and bicarbonate transporter (Phatr3_Jdraft1806).

(A) Relative reactive oxygen species (ROS) level detected by DCFH-DA fluorescent probe. All DCF intensity data were normalized to corresponding cell density (OD) and compared to the WT in seed culture. DCFH-DA, 2′, 7′-dichlorofluorescein diacetate; DCF, 2′-7′dichlorofluorescein.

(B) Intracellular superoxide dismutase (SOD) activity. DW stands for an estimated dry weight based on OD. Data are represented as mean ± standard deviation (n = 3). Two-factorial ANOVA was used to analyze ROS level and SOD activity, showing significant differences ($p < 0.05$) among different strains.

genes involving the TCA cycle were generally upregulated in all three transgenic strains, including 2-oxoglutarate dehydrogenase, succinate dehydrogenase, isocitrate lyase, malate synthase, and aconitase. However, the expression of a citrate synthase gene (Phatr3_J54477) was markedly decreased (Figure 5E). Due to the great demand for protein turnover, nitrogen assimilation mechanisms were explored, which revealed wide downregulation of nitrate, ammonium, and urea transporters in the WT and PtFDX-OE10. By contrast, many of these genes remained unchanged or upregulated in PtCPA-OE21 and PtSLC-OE31 (Figure 5E).

Transcriptomic profiles of transgenic strains

To uncover the molecular basis associated with phenotypical changes in the genetically modified strains, further analysis was conducted to study the relative expression between transgenics and WT at the same time points. Under non-stressed condition (pH8.0), transgenic strains had little difference from the WT (Table S3), except for PtCPA-OE21, which exhibited 1620 DEGs (Figure S4). Consequently, enrichment analyses based on DEGs revealed limited differential functions under non-stressed conditions. In PtFDX-OE10, a group was enriched with five sulfur compound binding proteins (GO:1901681), where two homologous genes (Phatr3_J16343, Phatr3_EG01877) of iron storage ferritins[48] were upregulated, which could be responsible for increasing production of [2Fe-2S]-containing FDXs. Additionally, these results suggested that overexpression of the solute:proton antiporter (Phatr_J50516) led to changes in protein metabolism with increased nitrogen assimilation (KEGG:00910) and hydrolysis of an amine group (GO:0016810), but functions related to protein translation/biosynthesis (GO:0006520) were downregulated. By contrast, a few GO terms were found enriched in PtSLC-OE31 under the acidic stress condition, which did not reveal the obvious impacts of overexpressing SCL4-2 (Phatr3_Jdraft1806) on cellular metabolism in this condition.

Against the WT, PtCPA-OE21 and PtSLC-OE31 in response to acidic stress differentially expressed 4,111 and 2,468 genes, respectively, whereas PtFDX-OE10 possessing 1,638 DEGs was less differentiated from the WT. According to GO enrichment results, PtFDX-OE10 in the low-pH treatment only functioned differently in limited biological processes, including DNA integration (GO:0015074) and amino acid metabolic process (GO:0006520). Although many GO terms were only enriched in either PtCPA-OE21 or PtSLC-OE31, gene expression patterns in these functions were found alike in both strains, which reflects similar growth performances under acidic stress. Relative changes in PtCPA-OE21 and PtSLC-OE31 are illustrated in Figure 6C. As a response to low-pH stress, transcription of many heat shock transcription factors was increased in PtCPA-OE21 and PtSLC-OE31. Importantly, many transmembrane transporters (GO:0055085) showed enhanced expression, which did not occur in PtFDX-OE10. For instance, solute carrier family 4 bicarbonate transporters, ABC transporters, potassium channel, P-type ATPase, nitrogen transporters, and ammonium transporters were likely to contribute to low-pH tolerance. Also, PtCPA-OE21 and PtSLC-OE31 shared multiple upregulated genes in nitrogen metabolism (KEGG:00910), propanoate metabolism (KEGG:00640), and pentose-phosphate shunt (GO:0006098). Furthermore, many genes functioning in chlorophyll-binding (GO:0016168), tetrapyrrole biosynthetic process (GO:0033014), and small-molecule biosynthetic process (GO:0044283) were downregulated in comparison with the WT. Also, lower expression was observed in multiple genes delivering fatty acid synthase activity (GO:0004312) and peroxidative activity (GO:0004601).

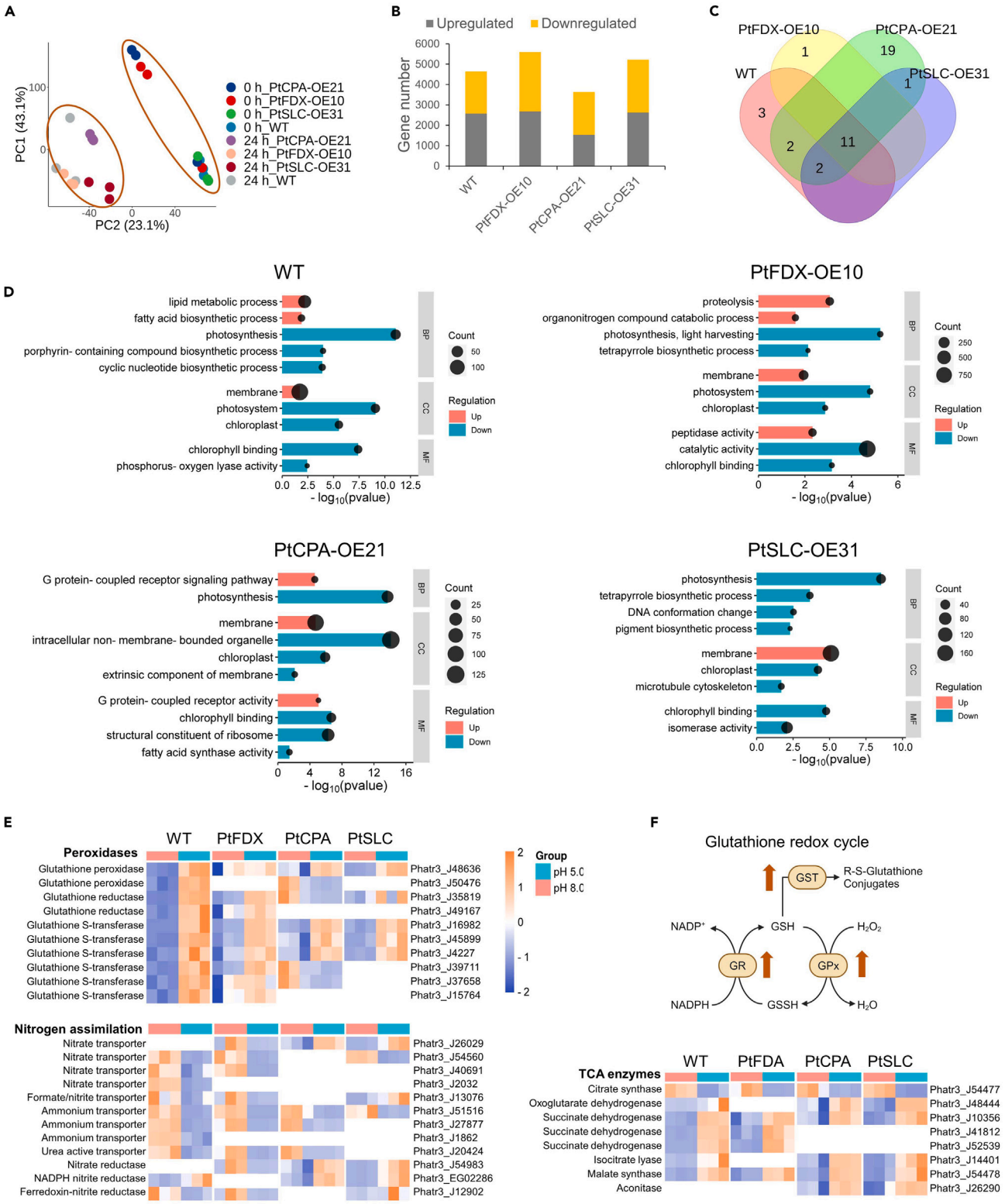

Figure 5. Effect of low-pH stress on gene expression in WT and transgenic strains

(A) Principal-component analysis (PCA) of gene expression (FPKM, fragments per kilobase of transcript per million fragments mapped) in different strains at 0 h (pH 8.0) and 24 h (pH 5.0).

Figure 5. *Continued*

(B) The number of differentially expressed genes (DEG) comparing the transcriptomes ($n = 3$) after 24 h's low-pH treatment (pH 5.0) and the control (pH 8.0) at 0 h.

(C) Comparison of enriched Gene Ontology (GO) terms among different strains. The values indicate numbers of intersecting GO terms.

(D) Highlighted driver GO terms (at least one function being presented from every connected component) under low-pH stress. GO categories include BP, biological process; CC, cellular component; MF, molecular function. The count stands for the number of enriched genes in a GO term.

(E) Expression patterns of genes involving glutathione metabolic process and nitrogen assimilation.

(F) Upregulated glutathione redox cycle in response to low-pH stress in WT. GPx, glutathione peroxidase; GR, glutathione reductase; GST, glutathione S-transferase; GSH, glutathione; GSSH, glutathione disulfide.

DISCUSSION

This study aims to improve acidic tolerance in diatoms. The model marine diatom *P. tricornutum* was engineered to overexpress PtFDX (Phatr3_J33543), PtCPA (Phatr3_J50516), and PtSLC4-2 (Phatr3_Jdraft1806). Our results indicate that these genetic modifications effectively enable the ability of *P. tricornutum* to withstand severe low-pH stress, as supported by improvements in photosynthetic function and oxidative stress responses. Despite the compromised photosynthetic efficiency caused by the acidic treatment, the inhibitory effect of low-pH was somewhat alleviated in transgenic strains, resulting in significantly higher photosynthetic quantum yields (Figure 3). According to the photochemistry model, maximal quantum yield (Fv/Fm) evaluates the potential efficiency of utilizing absorbed light for driving electron transfer from the reaction center chlorophyll to the primary quinone acceptor of photosystem II (Q_A). Stressful conditions lead to an increase in energy dissipation as heat, i.e., NPQ rather than photochemistry, thereby decreasing the maximal fluorescence potential (Fm). Hence, Fv/Fm in general should be reversely related to NPQ.[49] However, our results for transgenic strains showed higher values in both Fv/Fm and NPQ, but NPQ in the WT was unexpectedly kept low. These results indicate that the transgenic strains not only conducted relatively more efficient energy utilization for photochemistry but also dissipated more energy as heat. A possible explanation is that energy capture in the WT may have been impaired at the onset of low-pH treatment, resulting in an insufficient energy supply to support downstream photochemistry and heat dissipation.

Moreover, elevated generation of ROS serving as a signaling mechanism is a typical physiological response to environmental stresses, but excessive levels of ROS can be lethal to cells, causing damage to macromolecules such as lipids, proteins, and DNA.[50] In this study, the growth performances of different strains exhibited a clear correlation with their intracellular ROS levels. Whereas the WT *P. tricornutum* suffering from oxidative stress was severely inhibited at pH 5.0, the transgenic strains with significantly lower ROS levels showed positive growth. While ROS levels in both PtCPA-OE21 and PtSLC-OE31 remained low during cultivation, oxidative stress in PtFDX-OE10 increased over time, potentially contributing to the cell density after 24 h (Figure S3). The increasing trend in SOD activities observed in the WT and PtFDX-OE10 may be triggered by the increase in ROS levels. Furthermore, significantly lowered ROS levels in both PtFDX-OE10 and PtCPA-OE21 may be attributed to the higher initial antioxidant capacity provided by antioxidants such as SOD in the seed culture. Despite its SOD activity being low, PtSLC-OE31 was able to maintain a low ROS level. These results suggest that the enhanced expression of PtFDX may mitigate ROS by stimulating antioxidant-mediated detoxification, which however had limited resistance against the acidic stress for a prolonged period. In the other two transgenic strains, PtCPA and PtSLC4-2 which overexpress proton and bicarbonate transporters, respectively, alternative mechanisms apart from antioxidants may be involved in alleviating oxidative stress or preventing ROS generation.

Despite the demonstrated effective functions of the genetic modifications in enhancing acidic tolerance, the positive growth of transgenic strains ceased after 24 h. To address this issue, gene expression at pH 5.0 was further examined by qPCR and western blot. The transcripts of the recombinant genes, which were redesigned through codon optimization, could be differentiated from the transcripts of the corresponding native genes. The native genes in different strains showed varying levels of expression in response to low pH (Table 1). Both qPCR and transcriptomic data confirmed the successful transcription of these transgenes at high levels (Figure S5). Due to the pH-dependent property of EGFP,[51] the expression of the recombinant proteins could not be confirmed by detecting EGFP signals in acidic cultures. Anti-EGFP antibody was used in western blot to detect the presence of recombinant proteins in transgenic strains. While the WT (control) was absence of targeted protein signals, recombinant proteins were detectable by the anti-GFP antibody in all transgenic strains cultured in optimal conditions (pH 8.0). Furthermore, these proteins remained present after incubation at pH 5.0 for 24 h (Figure S5), confirming translation of the target proteins in the respective transgenic strains. Since stress tolerance is a complex response that involves the integration of multiple pathways, the impact of genetic modifications on a single gene might be limited. Interestingly, the predicted protein lengths of PtCPA and PtSLC4-2 were 115 kD (kilodalton) and 95 kD, respectively; they were not present at the expected sizes and exhibited multiple bands of varying sizes. This observation suggests the occurrence of mRNA alternative splicing during their expression.[52]

To resist the low-pH stress, transcriptomic responses revealed common reactions in all three transgenic strains including enhanced heat shock responses, proteasomal protein catabolism, chaperone-mediated protein folding/repair, TCA cycle, fatty acid biosynthesis, and defensive mechanisms such as glutathione metabolism. As environmental pH proportionally impacts the intracellular pH of diatom,[53] the drop of pH leading to the misfolding of proteins would likely induce the refolding and turnover of denatured protein to preserve cellular functions. Furthermore, there was a general upregulation of enzymes involved in the TCA cycle, indicating an elevated energy demand (Figure 5E). The upregulation of acetyl-CoA carboxylase (Phatr3_J55209), which catalyzes the initial step of fatty acid synthesis, was observed in all three transgenic strains, indicating an increased carbon flux directed toward lipid production. ROS-mediated lipid accumulation as a stress response for energy storage, membrane reconfiguration, and ROS scavenging has been widely reported in oleaginous microorganisms.[54] The upregulation of multiple fatty acid desaturases (Phatr3_J46383, Phatr3_J54219, Phatr3_J9316, Phatr3_J25769, Phatr3_J41570) suggests an increased formation of unsaturated fatty acids that may act as antioxidants to balance the ROS level.[54] Additionally, peroxidase-mediated defenses,

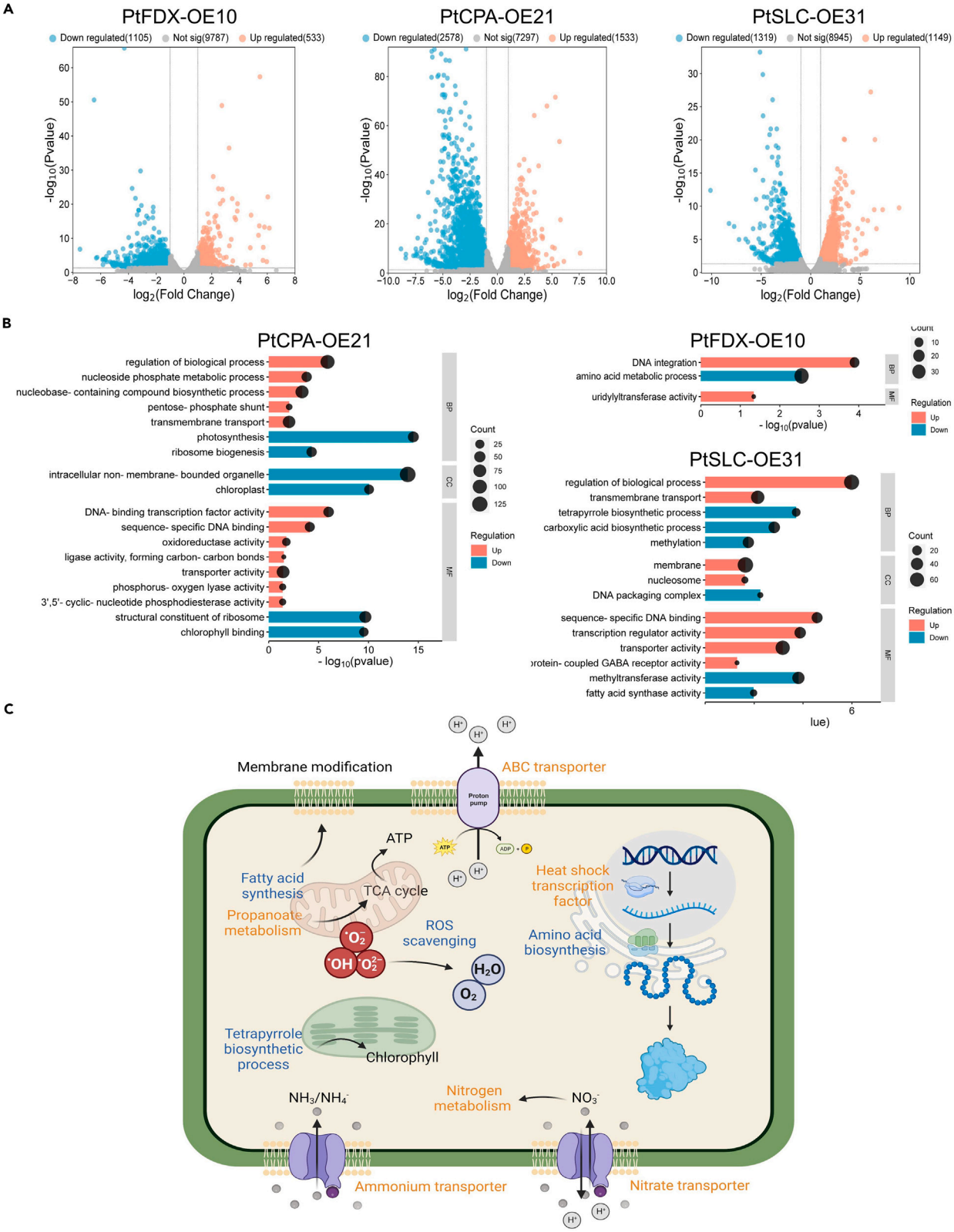
A
PtFDX-OE10
Down regulated(1105)
Not sig(9787)
Up regulated(533)
PtCPA-OE21
Down regulated(2578)
Not sig(7297)
Up regulated(1533)
PtSLC-OE31
Down regulated(1319)
Not sig(8945)
Up regulated(1149)
-log10(Pvalue)
log2(Fold Change)
B
PtCPA-OE21
regulation of biological process
nucleoside phosphate metabolic process
nucleobase- containing compound biosynthetic process
pentose- phosphate shunt
transmembrane transport
photosynthesis
ribosome biogenesis
intracellular non- membrane- bounded organelle
chloroplast
DNA- binding transcription factor activity
sequence- specific DNA binding
oxidoreductase activity
ligase activity, forming carbon- carbon bonds
transporter activity
phosphorus- oxygen lyase activity
3',5'- cyclic- nucleotide phosphodiesterase activity
structural constituent of ribosome
chlorophyll binding
BP
CC
MF
Count
Regulation
Up
Down
- log10(pvalue)
PtFDX-OE10
DNA integration
amino acid metabolic process
uridylyltransferase activity
PtSLC-OE31
regulation of biological process
transmembrane transport
tetrapyrrole biosynthetic process
carboxylic acid biosynthetic process
methylation
membrane
nucleosome
DNA packaging complex
sequence- specific DNA binding
transcription regulator activity
transporter activity
methyltransferase activity
fatty acid synthase activity
C
Membrane modification
ABC transporter
Proton pump
ATP
ADP
Fatty acid synthesis
TCA cycle
Propanoate metabolism
ROS scavenging
Heat shock transcription factor
Amino acid biosynthesis
Tetrapyrrole biosynthetic process
Chlorophyll
Nitrogen metabolism
NH3/NH4+
NO3-
Ammonium transporter
Nitrate transporter

Figure 6. Relative gene expression comparing transgenic strains with the WT

(A) Volcano plots presenting differentially expressed genes (DEGs) in transgenic strains at pH 5.0, using the WT as the control (n = 3).

(B) Highlighted driver Gene Ontology (GO) terms in transgenic strains. Highlighted driver GO terms have at least one function being presented from every connected component. GO categories include BP, biological process; CC, cellular component; MF, molecular function. The count stands for the number of enriched genes in a GO term.

(C) Schematic illustration of differentially expressed pathways based on findings in PtCPA-OE21 and PtSLC-OE31 (orange color indicates upregulation, blue color indicates downregulation).

especially the glutathione metabolic process, were generally provoked in all three transgenic strains to resolve the stress-induced ROS. Transcript abundance of a catalase-peroxidase (Phatr3_J18572) was elevated by 61.8-fold in the WT, underscoring the importance of this antioxidant in countering H^+ toxicity. This enzyme was also upregulated in all three transgenic strains in response to low-pH, albeit with much lower fold changes i.e., 15.9-folds in PtFDX-OE10, 2.5-folds in PtCPA-OE21, and 10.9-folds in PtSLC-OE31. In addition to the different expression patterns of glutathione redoxes, these results suggest fewer demands of peroxidase activities in the genetically modified strains, which is consistent with the results of intracellular ROS assay. Another common reaction to low-pH was the downregulation of genes related to light harvesting, e.g., chlorophyll-binding proteins, and pigment biosynthesis, e.g., chlorophyll and carotenoid. This phenomenon was also observed in our previous ALE experiments[19] suggesting a potential defense strategy to restrict ROS generation resulting from excessive electron flow.[55]

Further comparison of transcriptome profiles between transgenic strains and the WT found relatively similar expression patterns between the WT and PtFDX-OE10, whereas gene expression in PtCPA-OE21 and PtSLC-OE31 significantly differed from the WT (Figure 6A). These results imply that PtCPA-OE21 and PtSLC-OE31 share molecular features that could confer superior low-pH tolerance on them compared to WT and PtFDX-OE10. Examination of DEGs among different strains revealed higher expression of various transmembrane transporters in PtCPA-OE21 and PtSLC-OE31. Therein, ABC transporters and P-type ATPases were likely to participate in proton efflux and translocation. Additionally, elevated ammonium transporters and bicarbonate transporters (paralogs of PtSLC4-2) could assist in pH control by absorbing alkaline compounds such as NH_3/NH_4^- and HCO_3^-.[56] The upregulation of multiple nitrate transporters as well as nitrate and nitrite reductases was likely necessary for nitrogen assimilation to support protein synthesis. However, amino acid metabolism and translation machinery were found slightly downregulated in PtCPA-OE21 and PtSLC-OE31 (Figure 6). Therefore, nitrate/nitrite transporters and reductases may also contribute to proton translocation. In addition to the nitrate-reduction activity, the membrane-bound nitrate reductase plays a role in translocating cytoplasmic protons into periplasm.[57] Furthermore, nitrate uptake through nitrate transporter has been shown to alleviate H^+ toxicity in plants by increasing pH in the root's rhizosphere,[58] which may also apply to diatoms. The differential expression analysis among strains also revealed extensive lower expression of peroxidase systems in PtCPA-OE21 and PtSLC-OE31, including catalase, ascorbate peroxidase, GP_X, and SOD, in PtCPA-OE21 and PtSLC-OE31, thereby confirming the fact that ROS scavenging was not an immediate requirement in these strains (Figure 6C). Based on these results, we may propose that ROS generation was avoided in PtCPA-OE21 and PtSLC-OE31 by vast upregulation of transporters that could alleviate the impact of protons. The overexpression of Phatr_J33543 resulted in minimal changes in gene expression in response to the environmental change, as expected for a single modification on a non-regulatory gene. In contrast, the overexpression of a proton pump (Phatr_J50516) and a bicarbonate pump (Phatr_Jdraft1806) led to more extensive changes in the gene expression patterns, affecting numerous mechanisms and pathways (Table S4). These results imply that the direct effects of overexpressing Phatr_J50516 and Phatr_Jdraft1806 could induce fundamental changes, for example, cellular homeostasis that in turn could mediate signaling for global regulation.

The present study elucidated the critical roles of ion/electron carrier genes (Phatr3_J33543, Phatr3_J50516, and Phatr3_Jdraft1806) in conferring low-pH resistance to the model marine diatom *P. tricornutum*. These genetic modifications enabled the growth of *P. tricornutum* under an inhibitory low-pH stress. Physiological and molecular data suggested that these genes functioned differently in stress tolerance by either alleviating oxidative stress or preventing ROS generation. This study represents the initial endeavor to genetically engineer diatoms, based on an ALE approach integrated with a whole-genome transcriptomics analysis, for resistance against inhibitory acidic conditions. We anticipate that the proposed rational engineering strategy will expedite the advancement of robust transgenic microalgae for turning waste flue gas into valuable algal products, thereby contributing to the attainment of carbon neutrality and thus achievement of United Nations Sustainable Development Goals (UNSDGs) concerning climate action (SDG13) and energy security (SDG7).

Table 1. Differential expression (log_2FoldChange) of native genes of Phatr3_J33543 (PtFDX), Phatr3_J50516 (PtCPA), and Phatr3_Jdraft1806 (SLC4-2) in response to low-pH treatment in different strains (P_{adj} < 0.05)

Gene ID	Protein	WT	PtFDX-OE10	PtCPA-OE21	PtSLC-OE31
Phatr_J33543	Ferredoxin (FDX)	1.92	2.37	0.41*	2.23
Phatr_J50516	Cation/proton antiporter (CPA)	−1.11	−0.39*	0.00*	0.49*
Phatr_Jdraft1806	Solute carrier (SLC-2)	−0.25*	0.38*	−3.49	−2.75

(* represents non-significant changes, P_{adj} > 0.05).

The data represent relative changes comparing different pH treatments (pH5.0/pH8.0) using pH 8.0 as the control.

Limitation of the study

Given the engineering-focused nature of this study, one limitation is that functions of the targeted genes have not been fully elucidated through silencing or knockout modifications, which should be investigated in the future research. PtCPA and PtSLC4-2 are anticipated to directly participate in ion pumping. However, due to technological limitations, we could not measure intracellular pH or the pH of subcellular compartments. Instead, physiological impacts of overexpressing these transmembrane transporters were only demonstrated by indirect evidence, i.e., oxidative stress. Furthermore, overexpressing these transporters surprisingly had widespread effects on transcriptomes. We attribute this phenomenon to their influence on intracellular pH homeostasis. However, without measuring intracellular pH, we cannot confirm this hypothesis by showing whether genetic modifications maintained pH balance within the cells.

STAR★METHODS

Detailed methods are provided in the online version of this paper and include the following:

- KEY RESOURCES TABLE
- RESOURCE AVAILABILITY
  - Lead contact
  - Materials availability
  - Data and code availability
- EXPERIMENTAL MODEL AND STUDY PARTICIPANT DETAILS
  - Microbe strains
- METHOD DETAILS
  - Expression vector construction, electroporation, and transformant screening
  - Molecular characterization of the selected transformants
  - Growth and photosynthesis performances
  - Stress assessment
  - RNA extraction and library construction
  - RNA sequencing and transcriptomic analysis
- QUANTIFICATION AND STATISTICAL ANALYSIS

SUPPLEMENTAL INFORMATION

Supplemental information can be found online at https://doi.org/10.1016/j.isci.2024.110482.

ACKNOWLEDGMENTS

This study was supported by the National Natural Science Foundation of China Joint Fund Project (grant no. U23A2034), Hundred Talents Program of Zhejiang University, Science Foundation of Donghai Laboratory (grant no. DH-2022KF0203), Key Scientific Research and Development Program of Hangzhou (grant no. 202204T14), Icelandic Research Fund (grant no. 207298-052), and Technology Development Fund (grant no. 163922-0613)

AUTHOR CONTRIBUTIONS

Y.S. and W.F. designed the study. Y.S., J.C., J.H., C.Q., and J.M. conducted the experiments. Y.S. analyzed data and wrote the paper. S.B. and W.F. secured funding. J.C., J.H., C.Q., and J.M. reviewed the manuscript.

DECLARATION OF INTERESTS

The authors declare no competing interests.

Received: January 2, 2024
Revised: May 14, 2024
Accepted: July 8, 2024
Published: July 10, 2024

REFERENCES

1. Tarafdar, A., Sowmya, G., Yogeshwari, K., Rattu, G., Negi, T., Awasthi, M.K., Hoang, A., Sirohi, R., and Sirohi, R. (2023). Environmental pollution mitigation through utilization of carbon dioxide by microalgae. Environ. Pollut. *328*, 121623.

2. Olabi, A., Shehata, N., Sayed, E.T., Rodriguez, C., Anyanwu, R.C., Russell, C., and Abdelkareem, M.A. (2023). Role of microalgae in achieving sustainable development goals and circular economy. Sci. Total Environ. *854*, 158689.

3. Nagappan, S., Tsai, P.-C., Devendran, S., Alagarsamy, V., and Ponnusamy, V.K. (2020). Enhancement of biofuel production by microalgae using cement flue gas as substrate. Environ. Sci. Pollut. Res. Int. *27*, 17571–17586.

4. Van Den Hende, S., Vervaeren, H., and Boon, N. (2012). Flue gas compounds and microalgae:(Bio-) chemical interactions leading to biotechnological opportunities. Biotechnol. Adv. *30*, 1405–1424.
5. Aslam, A., Thomas-Hall, S.R., Mughal, T.A., and Schenk, P.M. (2017). Selection and adaptation of microalgae to growth in 100% unfiltered coal-fired flue gas. Bioresour. Technol. *233*, 271–283.
6. Song, Y., Cheng, J., Miao, Y., Guo, W., and Zhou, J. (2021). SO_2 impurity in simulated flue gas with 15% CO_2 affects dynamic bubble dissolution and arthrospira photosynthetic growth. ACS Sustain. Chem. Eng. *9*, 5580–5589.
7. Fu, J., Huang, Y., Xia, A., Zhu, X., Zhu, X., Chang, J.-S., and Liao, Q. (2022). How the sulfur dioxide in the flue gas influence microalgal carbon dioxide fixation: From gas dissolution to cells growth. Renew. Energy *198*, 114–122.
8. Pawlowski, A., Mendoza, J., Guzmán, J., Berenguel, M., Acién, F., and Dormido, S. (2014). Effective utilization of flue gases in raceway reactor with event-based pH control for microalgae culture. Bioresour. Technol. *170*, 1–9.
9. Xie, M., Qiu, Y., Song, C., Qi, Y., Li, Y., and Kitamura, Y. (2018). Optimization of *Chlorella sorokiniana* cultivation condition for simultaneous enhanced biomass and lipid production via CO_2 fixation. Bioresour. Technol. Rep. *2*, 15–20.
10. Jin, X., Gong, S., Chen, Z., Xia, J., and Xiang, W. (2021). Potential microalgal strains for converting flue gas CO_2 into biomass. J. Appl. Phycol. *33*, 47–55.
11. Cheng, J., Zhu, Y., Zhang, Z., and Yang, W. (2019). Modification and improvement of microalgae strains for strengthening CO_2 fixation from coal-fired flue gas in power plants. Bioresour. Technol. *291*, 121850.
12. Kao, C.-Y., Chiu, S.-Y., Huang, T.-T., Dai, L., Wang, G.-H., Tseng, C.-P., Chen, C.-H., and Lin, C.-S. (2012). A mutant strain of microalga *Chlorella* sp. for the carbon dioxide capture from biogas. Biomass Bioenergy *36*, 132–140.
13. Fu, W., Guðmundsson, Ó., Paglia, G., Herjólfsson, G., Andrésson, Ó.S., Palsson, B.Ø., and Brynjólfsson, S. (2013). Enhancement of carotenoid biosynthesis in the green microalga *Dunaliella salina* with light-emitting diodes and adaptive laboratory evolution. Appl. Microbiol. Biotechnol. *97*, 2395–2403.
14. Fu, W., Gudmundsson, O., Feist, A.M., Herjolfsson, G., Brynjolfsson, S., and Palsson, B.Ø. (2012). Maximizing biomass productivity and cell density of *Chlorella vulgaris* by using light-emitting diode-based photobioreactor. J. Biotechnol. *161*, 242–249.
15. Choi, H.I., Hwang, S.-W., Kim, J., Park, B., Jin, E., Choi, I.-G., and Sim, S.J. (2021). Augmented CO_2 tolerance by expressing a single H^+-pump enables microalgal valorization of industrial flue gas. Nat. Commun. *12*, 6049.
16. Ong, S.-C., Kao, C.-Y., Chiu, S.-Y., Tsai, M.-T., and Lin, C.-S. (2010). Characterization of the thermal-tolerant mutants of *Chlorella* sp. with high growth rate and application in outdoor photobioreactor cultivation. Bioresour. Technol. *101*, 2880–2883.
17. Kuo, C.-M., Lin, T.-H., Yang, Y.-C., Zhang, W.-X., Lai, J.-T., Wu, H.-T., Chang, J.-S., and Lin, C.-S. (2017). Ability of an alkali-tolerant mutant strain of the microalga *Chlorella* sp. AT1 to capture carbon dioxide for increasing carbon dioxide utilization efficiency. Bioresour. Technol. *244*, 243–251.
18. Barten, R., Peeters, T., Navalho, S., Fontowicz, L., Wijffels, R.H., and Barbosa, M. (2022). Expanding the upper-temperature boundary for the microalga *Picochlorum* sp.(BPE23) by adaptive laboratory evolution. Biotechnol. J. *17*, 2100659.
19. Su, Y., Xu, M., Brynjólfsson, S., and Fu, W. (2023). Physiological and molecular insights into adaptive evolution of the marine model diatom *Phaeodactylum tricornutum* under low-pH stress. J. Clean. Prod. *412*, 137297.
20. Siripornadulsil, S., Traina, S., Verma, D.P.S., and Sayre, R.T. (2002). Molecular mechanisms of proline-mediated tolerance to toxic heavy metals in transgenic microalgae. Plant Cell *14*, 2837–2847.
21. Castell, C., Bernal-Bayard, P., Ortega, J.M., Roncel, M., Hervás, M., and Navarro, J.A. (2021). The heterologous expression of a plastocyanin in the diatom *Phaeodactylum tricornutum* improves cell growth under iron-deficient conditions. Physiol. Plant. *171*, 277–290.
22. Ye, G.-B., Qin, Z.-H., Bin, X.-Y., Mou, J.-H., Lin, C.S.K., Li, H.-Y., and Wang, X. (2022). 3-Oxoacyl acyl carrier protein reductase overexpression reveals its unprecedented roles in biofuel production and high-temperature tolerance in diatom. J Fuel *325*, 124844.
23. Celi, C., Fino, D., and Savorani, F. (2022). *Phaeodactylum tricornutum* as a source of value-added products: A review on recent developments in cultivation and extraction technologies. Bioresour. Technol. Rep. *19*, 101122.
24. Bowler, C., Allen, A.E., Badger, J.H., Grimwood, J., Jabbari, K., Kuo, A., Maheswari, U., Martens, C., Maumus, F., Otillar, R.P., et al. (2008). The *Phaeodactylum* genome reveals the evolutionary history of diatom genomes. J Nature *456*, 239–244.
25. Butler, T., Kapoore, R.V., and Vaidyanathan, S. (2020). *Phaeodactylum tricornutum*: a diatom cell factory. Trends Biotechnol. *38*, 606–622.
26. Jiang, X., Zhu, B., Tu, C., Li, Y., Zhao, Y., Yang, G., and Pan, K. (2022). Silencing 1, 3-β-glucan synthase gene promotes total lipid production and changes fatty acids composition by affecting carbon flow distribution in *Phaeodactylum tricornutum*. Algal Res. *67*, 102827.
27. Cen, S.-Y., Li, D.-W., Huang, X.-L., Huang, D., Balamurugan, S., Liu, W.-J., Zheng, J.-W., Yang, W.-D., and Li, H.-Y. (2022). Crucial carotenogenic genes elevate hyperaccumulation of both fucoxanthin and β-carotene in *Phaeodactylum tricornutum*. Algal Res. *64*, 102691.
28. Zhang, R., Zhu, B., Tu, C., Li, Y., Zhao, Y., and Pan, K. (2021). The combined effect of nitrogen deprivation and overexpression of malic enzyme gene on growth and lipid accumulation in *Phaeodactylum tricornutum*. J. Appl. Phycol. *33*, 3637–3645.
29. Seo, S., Jeon, H., Chang, K.S., and Jin, E. (2018). Enhanced biomass production by *Phaeodactylum tricornutum* overexpressing phosphoenolpyruvate carboxylase. J. Algal Research *31*, 489–496.
30. Seo, S., Kim, J., Lee, J.-W., Nam, O., Chang, K.S., and Jin, E. (2020). Enhanced pyruvate metabolism in plastids by overexpression of putative plastidial pyruvate transporter in *Phaeodactylum tricornutum*. Biotechnol. Biofuels *13*, 120–211.
31. Nakajima, K., Tanaka, A., and Matsuda, Y. (2013). SLC4 family transporters in a marine diatom directly pump bicarbonate from seawater. Proc. Natl. Acad. Sci. USA *110*, 1767–1772.
32. Hanke, G., and Mulo, P. (2013). Plant type ferredoxins and ferredoxin-dependent metabolism. Plant Cell Environ. *36*, 1071–1084.
33. Huang, L.-F., Lin, J.-Y., Pan, K.-Y., Huang, C.-K., and Chu, Y.-K. (2015). Overexpressing ferredoxins in Chlamydomonas reinhardtii increase starch and oil yields and enhance electric power production in a photo microbial fuel cell. Int. J. Mol. Sci. *16*, 19308–19325.
34. Lin, Y.-H., Pan, K.-Y., Hung, C.-H., Huang, H.-E., Chen, C.-L., Feng, T.-Y., and Huang, L.-F. (2013). Overexpression of ferredoxin, PETF, enhances tolerance to heat stress in *Chlamydomonas reinhardtii*. Int. J. Mol. Sci. *14*, 20913–20929.
35. Tsujii, M., Tanudjaja, E., and Uozumi, N. (2020). Diverse physiological functions of cation proton antiporters across bacteria and plant cells. Int. J. Mol. Sci. *21*, 4566.
36. Bassil, E., Tajima, H., Liang, Y.-C., Ohto, M.-a., Ushijima, K., Nakano, R., Esumi, T., Coku, A., Belmonte, M., and Blumwald, E. (2011). The Arabidopsis Na^+/H^+ antiporters NHX1 and NHX2 control vacuolar pH and K^+ homeostasis to regulate growth, flower development, and reproduction. Plant Cell *23*, 3482–3497.
37. Xie, Q., Zhou, Y., and Jiang, X. (2022). Structure, function, and regulation of the plasma membrane Na+/H+ antiporter salt overly sensitive 1 in plants. Front. Plant Sci. *13*, 866265.
38. Wang, B., Zhai, H., He, S., Zhang, H., Ren, Z., Zhang, D., and Liu, Q. (2016). A vacuolar Na^+/H^+ antiporter gene, IbNHX2, enhances salt and drought tolerance in transgenic sweetpotato. Sci. Hortic. *201*, 153–166.
39. Shimamoto, T., Inaba, K., Thelen, P., Ishikawa, T., Goldberg, E.B., Tsuda, M., and Tsuchiya, T. (1994). The NhaB Na^+/H^+ antiporter is essential for intracellular pH regulation under alkaline conditions in Escherichia coli. J. Biochem. *116*, 285–290.
40. Quinn, M.J., Resch, C.T., Sun, J., Lind, E.J., Dibrov, P., and Häse, C.C. (2012). NhaP1 is a K^+ (Na^+)/H^+ antiporter required for growth and internal pH homeostasis of Vibrio cholerae at low extracellular pH. Microbiology *158*, 1094–1105.
41. Krulwich, T.A., Ito, M., and Guffanti, A.A. (2001). The Na^+-dependence of alkaliphily in Bacillus. Biochim. Biophys. Acta *1505*, 158–168.
42. Berge, T., Daugbjerg, N., Andersen, B.B., and Hansen, P.J. (2010). Effect of lowered pH on marine phytoplankton growth rates. Mar. Ecol. Prog. Ser. *416*, 79–91.
43. Nawaly, H., Matsui, H., Tsuji, Y., Iwayama, K., Ohashi, H., Nakajima, K., and Matsuda, Y. (2023). Multiple plasma membrane SLC4s contribute to external HCO_3^- acquisition during CO_2 starvation in the marine diatom *Phaeodactylum tricornutum*. J. Exp. Bot. *74*, 296–307.
44. Parks, S.K., and Pouyssegur, J. (2015). The Na^+/HCO_3^- co-transporter SLC4A4 plays a role in growth and migration of colon and breast cancer cells. J. Cell. Physiol. *230*, 1954–1963.

45. Hu, M.Y., Yan, J.-J., Petersen, I., Himmerkus, N., Bleich, M., and Stumpp, M. (2018). A SLC4 family bicarbonate transporter is critical for intracellular pH regulation and biomineralization in sea urchin embryos. Elife *7*, e36600.
46. Ruffin, V.A., Salameh, A.I., Boron, W.F., and Parker, M.D. (2014). Intracellular pH regulation by acid-base transporters in mammalian neurons. Front. Physiol. *5*, 43.
47. Raudvere, U., Kolberg, L., Kuzmin, I., Arak, T., Adler, P., Peterson, H., and Vilo, J. (2019). g: Profiler: a web server for functional enrichment analysis and conversions of gene lists (2019 update). Nucleic Acids Res. *47*, W191–W198.
48. Cohen, N.R., Mann, E., Stemple, B., Moreno, C.M., Rauschenberg, S., Jacquot, J.E., Sunda, W.G., Twining, B.S., and Marchetti, A. (2018). Iron storage capacities and associated ferritin gene expression among marine diatoms. Limnol. Oceanogr. *63*, 1677–1691.
49. Baker, N.R. (2008). Chlorophyll fluorescence: a probe of photosynthesis in vivo. Annu. Rev. Plant Biol. *59*, 89–113.
50. Schieber, M., and Chandel, N.S. (2014). ROS function in redox signaling and oxidative stress. Curr. Biol. *24*, R453–R462.
51. Roberts, T.M., Rudolf, F., Meyer, A., Pellaux, R., Whitehead, E., Panke, S., and Held, M. (2016). Identification and Characterisation of a pH-stable GFP. Sci. Rep. *6*, 28166.
52. Liu, Y., Yang, J., and Chen, L.-M. (2015). Structure and function of SLC4 family HCO_3^- transporters. Front. Physiol. *6*, 355.
53. Hervé, V., Derr, J., Douady, S., Quinet, M., Moisan, L., and Lopez, P.J. (2012). Multiparametric analyses reveal the pH-dependence of silicon biomineralization in diatoms. PLoS One *7*, e46722.
54. Shi, K., Gao, Z., Shi, T.-Q., Song, P., Ren, L.-J., Huang, H., and Ji, X.-J. (2017). Reactive oxygen species-mediated cellular stress response and lipid accumulation in oleaginous microorganisms: the state of the art and future perspectives. Front. Microbiol. *8*, 793.
55. Mus, F., Toussaint, J.-P., Cooksey, K.E., Fields, M.W., Gerlach, R., Peyton, B.M., and Carlson, R.P. (2013). Physiological and molecular analysis of carbon source supplementation and pH stress-induced lipid accumulation in the marine diatom *Phaeodactylum tricornutum*. Appl. Microbiol. Biotechnol. *97*, 3625–3642.
56. Yang, Q., Yang, Y., Tang, Y., Wang, X., Chen, Y., Shen, W., Zhan, Y., Gao, J., Wu, B., He, M., et al. (2020). Development and characterization of acidic-pH-tolerant mutants of *Zymomonas mobilis* through adaptation and next-generation sequencing-based genome resequencing and RNA-Seq. Biotechnol. Biofuels *13*, 144–217.
57. Kuypers, M.M., Marchant, H.K., and Kartal, B. (2018). The microbial nitrogen-cycling network. Nat. Rev. Microbiol. *16*, 263–276.
58. Fang, X.Z., Tian, W.H., Liu, X.X., Lin, X.Y., Jin, C.W., and Zheng, S.J. (2016). Alleviation of proton toxicity by nitrate uptake specifically depends on nitrate transporter 1.1 in Arabidopsis. New Phytol. *211*, 149–158.
59. Chu, L., Ewe, D., Bártulos, C.R., Kroth, P.G., and Gruber, A. (2016). Rapid induction of GFP expression by the nitrate reductase promoter in the diatom Phaeodactylum tricornutum. PeerJ *4*, e2344.
60. Berges, J.A., Franklin, D.J., and Harrison, P.J. (2001). Evolution of an artificial seawater medium: improvements in enriched seawater, artificial water over the last two decades. J. Phycol. *37*, 1138–1145.
61. Zhang, C., and Hu, H. (2014). High-efficiency nuclear transformation of the diatom Phaeodactylum tricornutum by electroporation. Mar. Genomics *16*, 63–66.
62. Chen, S., Zhou, Y., Chen, Y., and Gu, J. (2018). fastp: an ultra-fast all-in-one FASTQ preprocessor. J Bioinformatics *34*, i884–i890.
63. Kim, D., Langmead, B., and Salzberg, S.L. (2015). HISAT: a fast spliced aligner with low memory requirements. Nat. Methods *12*, 357–360.
64. Pertea, M., Pertea, G.M., Antonescu, C.M., Chang, T.-C., Mendell, J.T., and Salzberg, S.L. (2015). StringTie enables improved reconstruction of a transcriptome from RNA-seq reads. Nat. Biotechnol. *33*, 290–295.
65. Anders, S., Pyl, P.T., and Huber, W. (2015). HTSeq—a Python framework to work with high-throughput sequencing data. J Bioinformatics *31*, 166–169.

STAR★METHODS

KEY RESOURCES TABLE

REAGENT or RESOURCE	SOURCE	IDENTIFIER
Antibodies		
anti-GFP	Beyotime Biotech Inc	Cat#AG281; RRID: AB_2895206
anti-GAPDH	Beyotime Biotech Inc	Cat#AF0006; RRID: AB_2715590
Goat anti-mouse IgG	Beyotime Biotech Inc	Cat#A0216; RRID: AB_2860575
Chemicals, peptides, and recombinant proteins		
Ampicillin	Solarbio	Cas:69-52-3
Kanamycin	Biosharp	Cas:25389-94-0
Streptomycin	Biofrox	Cas:3810-74-0
Zeocin	Invitrogen	Cat#R25001
NdeI restriction enzyme	Takara	Cat#1161A
Sorbitol	Aladdin	Cat#D274374
MES (2-N-morpholinoethane-sulfonic acid)	Aladdin	Cas:145224-94-8
Tris-HCl	Rhawn	Cas:77-86-1
DCFH-DA(2′,7′-dichlorofluorescein diacetate)	Solarbio	Cat#CA1410
TRIzol reagent	Invitrogen	Cat#15596018
Critical commercial assays		
Monarch Plasmid Miniprep Kit	NEB	T1010S
EZNA HP Plant DNA Kit	Omega	D2485-01
DNA Clean & Concentrator	Zymo	D4013
Deposited data		
Transcriptomes of wild-type and transgenic strains in different conditions	This paper	NCBI: BioProject ID PRJNA1127795
Experimental models: Organisms/strains		
Phaeodactylum tricornutum	CCAP	1055/1
P.tricornutum: strain PtFDX-OE10	This paper	N/A
P.tricornutum: strain PtCPA-OE21	This paper	N/A
P.tricornutum: strain PtSLC-OE31	This paper	N/A
Oligonucleotides		
Primers used in this work	This paper	See Tables S2 and S5
Recombinant DNA		
pPhaNR	Chu et al.[59]	JN180663.1
PtFDX-EGFP	Sangon Biotech Co. Ltd	N/A
PtCPA-EGFP	Sangon Biotech Co. Ltd	N/A
PtSLC-EGFP	Sangon Biotech Co. Ltd	N/A
Software and algorithms		
MEGA11	MEGA Software	https://www.megasoftware.net/
Geneious Prime	Geneious	https://www.geneious.com/
Excel	Microsoft	http://www.office.com/
Other		
pH meter	Ohaus	Aquasearcher AB33M1

(*Continued on next page*)

Continued

REAGENT or RESOURCE	SOURCE	IDENTIFIER
Portable fluorometer	PSI	AquaPen-C
NanoDrop spectrophotometer	Thermo Scientific	NanoDrop 2000
Spectrophotometer	Hach	DR3900
Microplate reader	BioTek	Synergy H1
PCR cycler	Heal Force	GM-05

RESOURCE AVAILABILITY

Lead contact

Further inquiries and requests should be directed to the lead contact, Dr. Weiqi Fu (weiqifu@zju.edu.cn).

Materials availability

This study did not create new unique reagents. Requests for materials listed in key resources table should be directed to the lead contact.

Data and code availability

- The transcriptomic data has been deposited at NCBI and is publicly available as of the date of publication. Accession numbers are listed in the key resources table.
- This paper does not report original code.
- Any additional information required to reanalyze the data reported in this paper is available from the lead contact upon request.

EXPERIMENTAL MODEL AND STUDY PARTICIPANT DETAILS

Microbe strains

Axenic culture of the marine diatom *Phaeodactylum tricornutum* (CCAP 1055/1) was purchased from the Culture Collection of Algae and Protozoa (CCAP), Scotland, UK. The inoculum was grown in enriched artificial seawater (EASW)[60] at 22 ± 1°C under continuous illumination of red/blue (50:50) LED with a light intensity of 40 μmol m^{-2} s^{-1}. The EASW medium was supplemented with 40 mM Tris-HCl to maintain the pH of the media at 8.0. For low-pH treatments, 40 mM MES (2-N-morpholinoethane-sulfonic acid) buffer was applied to control the acidic pH range. Additionally, the medium was supplemented with ampicillin (100 μg mL^{-1}), kanamycin (100 μg mL^{-1}), and streptomycin (100 μg mL^{-1}) and sterilized by filtration using a 0.22 μm membrane filter (S-PAK, Millipore, US) to avoid bacterial contamination.

METHOD DETAILS

Expression vector construction, electroporation, and transformant screening

Target genes, Phatr3_J33543 (PtFDX), Phatr3_J50516 (PtCPA), and Phatr3_Jdraft1806 (PtSLC4-2) are 780 bp, 2588 bp, and 1913 bp of nucleotides in length, respectively. Their coding sequences (CDS) and amino acid sequences were retrieved from the European Molecular Biology Laboratory (EMBL) database. Homologous proteins were searched against the NCBI server (http://www.ncbi.nlm.nih.gov/) and filtered for >40% identity. Phylogenetic trees were constructed based on corresponding amino acid sequences using MEGA11 by the Maximum Likelihood algorithm. The conserved domains of each protein were identified using the NCBI CD-search tool.

The transgenic proteins (minus the stop codon) were fused to an enhanced green fluorescence protein (EGFP) at its N-terminus through a 5 × glycine linker (Figure 1A). The recombinant gene constructs were codon-optimized and artificially synthesized (Sangon Biotech Co. Ltd., China) and cloned into the multiple cloning sites of pPhaNR plasmid (NCBI accession: JN180663.1) under the control of the nitrate reductase promoter. After linearization by digestion at the NdeI restriction site, the overexpression vectors were introduced into diatom cells through electroporation according to a published protocol.[61] Following transformation, cells were spread onto EASW solid plates (1% w/v, agar) containing 100 μg mL^{-1} Zeocin (Invitrogen, US). In approximately three to four weeks visible colonies on the selective plates were transferred into liquid media containing Zeocin (100 μg mL^{-1}) and subcultured twice in microplates. Nitrate in the ESAW medium was enriched (4.4 mM) to ensure constitutively active expression of the transgenes. Successful transformants were initially screened by detecting EGFP signals against the wild-type (WT) strain using a microplate reader (BioTek, US), which was confirmed by observing green fluorescence under a microscope. Three transformants with strong fluorescent signals (one for each transgene), denoted as PtFDX-OE10, PtCPA-OE21, and PtSLC-OE31 for Phatr3_J33543, Phatr3_J50516, and Phatr3_Jdraft1806, respectively were selected for the following phenotype characterization.

Molecular characterization of the selected transformants

The presence of the target genes in the transformants was validated by genomic PCR amplifying the non-native recombinant fragments of the transgenic constructs (Figure 1A). Genomic DNA of transgenic strains was extracted using an HP Plant DNA Kit (Omega, USA) and

subsequently used as the templates in genomic PCR using the primer pairs listed in Table S1. Green fluorescence was detected by a microplate reader (BioTek, US) and fluorescent microscope at the excitation wavelength (λ_{ex}) of 488 nm and emission wavelength (λ_{em}) of 525 nm.

Growth and photosynthesis performances

Growths of the transformants (PtFDX-OE10, PtCPA-OE21, and PtSLC-OE31) were characterized in comparison with the WT strain by batch cultivation in flasks (250 mL) with 100 mL working volume. Three biological replicates were conducted for all growth experiments. Optimal growths of different strains were determined in the regular ESAW medium (pH 8.0), followed by low-pH treatment. For the transfer, cells in the exponential growth phase were pelleted by centrifugation at 1500 × g for 10 min (15°C) and washed once using acidic media (at pH 5.5 and pH 5.0, respectively). Then, cells were centrifuged again and resuspended into the corresponding buffered fresh ESAW media. The initial optical density (OD_{750}) of each group was adjusted to 0.050 ± 0.005.

Cell growth was monitored by measuring OD_{750} using a spectrophotometer (DR3900, Hach, US). The specific growth rate (μ, d^{-1}) was calculated using the following equation:

$$\mu = (\ln X_t - \ln X_0) / (t - t_0)$$

where X_t and X_0 are the OD at time t and the beginning of the time interval (t_0), respectively. Biomass dry weight (DW) was estimated based on an established correlation between OD_{750} and DW (mg mL^{-1}) as follows:

$$DW = 0.7429 \times OD_{750} \ (R^2 = 0.999)$$

For chlorophyll fluorescence determination, a 3 mL culture was incubated in the dark for 15 min. Photosynthetic parameters including maximum quantum yield (F_v/F_m), ΦPSII, and NPQ were measured with an AquaPen-C AP110 fluorometer (Photon Systems Instruments, Czech Republic) using the built-in program (non-photochemical quenching (NPQ) protocol 3).

Stress assessment

Intracellular ROS level was determined using the 2′, 7′-dichlorofluorescein diacetate (DCFH-DA) fluorescent probe. For each assay, an aliquot of 2μL DHCF-DA was added to a 200 μL cell sample (final concentration: 10 μM) and incubated at 37°C for 20 min in dark. Fluorescence at λ_{ex} = 488 nm and λ_{em} = 525 nm was measured with a microplate reader (BioTek, US). The results were presented as the ratio of fluorescence intensity at 525 nm normalized to cell density (OD_{750}) compared to the WT in control.

RNA extraction and library construction

Total RNA was extracted using the TRIzol reagent (Invitrogen, CA, USA) according to the manufacturer's protocol. RNA purity and quantification were evaluated using the NanoDrop 2000 spectrophotometer (Thermo Scientific, USA). RNA integrity was assessed using the Agilent 2100 Bioanalyzer (Agilent Technologies, Santa Clara, CA, USA). Then the libraries were prepared using VAHTS Universal V6 RNA-seq Library Prep Kit according to the manufacturer's instructions.

RNA sequencing and transcriptomic analysis

The transcriptome sequencing was conducted by OE Biotech Co., Ltd. (Shanghai, China) based on the Illumina Novaseq 6000 platform, generating 150 bp paired-end reads. After trimming by fastp,[62] the resulted clean reads data with >90% Q30 were mapped to the reference genome using Hisat2.[63] Following reads assembly by StringTie2,[64] gene structure extension and novel transcripts identification were performed by comparing the reference genome and the known annotated genes using Cuffcompare software. Fragments per kilobase of exon per million mapped fragments (FPKM) and read counts of each transcript (protein-coding gene) were calculated using HTSeq-count.[65]

By comparing transcriptomes from low-pH treatment/control for each strain and transgenic strains/WT at 0 h and 24 h timepoints, differentially expressed genes (DEGs) were identified using the DESeq (2012) R package. The RNAseq data was validated by qPCR using primers in Table S5 to detect expression levels of five randomly selected genes. The thresholds with adjusted *p*-value <0.05 and $|Log_2FoldChange| \geq 1$ were set for determining significant expression. Based on the hypergeometric distribution, Gene ontology (GO) enrichment analysis of DEGs was performed to reveal the significant enriched term (Padj <0.05) using the g:Profiler web server.[47]

QUANTIFICATION AND STATISTICAL ANALYSIS

All the growth, biochemical and molecular data of transgenic strains were compared to those of the WT. Statistical analyses were performed either using ANOVA (Analysis of Variance) or a two-tailed Student's t test on Microsoft Excel. All data were obtained from three independent biological replicates and reported as means ± standard deviation (n = 3).